Biosensors and Bioelectronics 26 (2011) 4040–4045

Contents lists available at ScienceDirect

Biosensors and Bioelectronics

journal homepage: www.elsevier.com/locate/bios

Electrochemical DNA biosensor for screening of chlorinated benzene pollutants

Lidong Wu [1], Xianbo Lu [1], Jing Jin, Haijun Zhang, Jiping Chen *

Dalian Institute of Chemical Physics, Chinese Academy of Sciences, Dalian 116023; Graduate School of Chinese Academy of Science, Beijing 100049, China

ARTICLE INFO

Article history:
Received 29 January 2011
Received in revised form 19 March 2011
Accepted 27 March 2011
Available online 2 April 2011

Keywords:
Chlorinated benzenes
Electrochemical oligonucleotide biosensor
Screening
Toxicity evaluation
Environmental monitoring

ABSTRACT

In this work, an electrochemical DNA biosensor based on double-stranded DNA modified Au electrode (dsDNA/Au) was proposed for the rapid screening and detection of chlorinated benzenes pollutants, in which redox-active methylene blue (MB) was used to amplify the interaction between dsDNA and the target analyte. Using hexachlorobenzene (HCB) as a model analyte of chlorinated benzenes, the biosensor demonstrated a linear response with the logarithm of HCB concentrations from 100 pmol L^{-1} to 100 nmol L^{-1}. The obtained detection limit was 30 pmol L^{-1}, which was remarkably superior to other biosensors. The interaction mechanism of the biosensor with HCB was proposed based on systematical characterization by cyclic voltammetry (CV), differential pulse voltammetry (DPV), UV–vis spectrometry and electrochemical quartz crystal microbalance (EQCM). Further studies revealed that the biosensor could screen chlorinated benzenes in the presence of 100 fold amount of other co-existing chemicals (ethyl acetate and sodium oxalate, etc.), and the response signal of the biosensors for different chlorinated benzenes was correlative to their respective toxicity. The proposed biosensor proved to be a promising "alarm" tool for rapid screening of chlorinated benzenes in real water samples.

1. Introduction

Chlorinated benzenes are persistent organic pollutants (POPs) which are formerly produced as fungicide and widely disseminated within the environment. These POPs (identified as probable human carcinogens by the International Agency for Research on Cancer) usually exist around the environment at the trace level, but inflict profound impacts on environmental security. These pollutants increasingly cause serious environmental problems because of bioaccumulation in some ecosystems and their mutagenic effects (Shin et al., 2010). Currently, these pollutants are usually determined by gas chromatography, high performance liquid chromatography or spectroscopy. Some of the current analytical techniques can achieve high resolution and good precision, but these techniques are time-consuming and complicated with cumbersome and costly instruments. Thus, there is a crucial need to develop new techniques which can rapidly screen these chlorinated benzenes pollutants in a selective and sensitive manner in order to enable remediation for the emergency contamination and unexpected accident in time.

The electrochemical oligonucleotide (E-DNA) biosensor may be an ideal alternative for pollutants screening and detection as they are cost-effective, fast and portable detection, which makes *in situ* and real time monitoring possible, without extensive and time-consuming sample preparation. Currently, E-DNA biosensor has been intensively developed with significant benefits in the rapid and cost-effective detection of specific DNA sequences based on DNA hybridization. Ariksoysal et al. developed a label-free electrochemical hybridization genosensor for the detection of hepatitis B virus (Ariksoysal et al., 2005). A series of studies devoted to using hybridization principle for viral (Ding et al., 2009) and microbial gene identification (Siddiquee et al., 2010), genetic disease diagnosis (Chen et al., 2008; Lin et al., 2007) and high throughput screening of environmental viral and microbial contaminants (Tombelli et al., 2009) have been reported. Another important application of E-DNA biosensor is for the screening of pollutants based on DNA affinity or DNA damage. Wang et al. developed a biosensor for screening hydrazine compounds by monitoring the changes in the anodic response of the double-stranded (ds) DNA-coated carbon paste electrode resulting from its interaction with hydrazine compounds (Wang et al., 1996). Limited efforts for monitoring environmental pollutants by E-DNA biosensor have been reported, such as naphthylamine, aflatoxin B1, arsenic trioxide and heavy metals (Lucarelli et al., 2002; Nowicka et al., 2010; Ozsoz et al., 2003). Up to date, the E-DNA biosensor for monitoring chlorinated benzenes has not been reported, although the screening and detection of chlorinated benzenes is a very important area in environment monitoring.

* Corresponding author at: Dalian Institute of Chemical Physics, Chinese Academy of Sciences, Dalian 116023, China. Tel.: +86 411 84379562; fax: +86 411 84379562.
E-mail address: chenjp@dicp.ac.cn (J. Chen).
[1] The authors contribute equally to this work.

0956-5663/$ – see front matter.
doi:10.1016/j.bios.2011.03.027

Moreover, for all these work mentioned above, the oxidation signals of guanine bases were used as analytical signals to detect these environmental pollutants. Owing to the limited amounts of guanine bases on oligonucleotide modified electrode, the response signals of these type of E-DNA biosensor were relatively poor and only mg L^{-1} of detection limits for analytes have been obtained (Rodriguez-Mozaz et al., 2006). Furthermore, the high guanine oxidation potential (typically 1.0–1.2 V) were prone to be affected by co-existing interferences, which further limited the improvement of their detection limits. As is well-documented, the amounts of environmental pollutants are usually at trace level. Thus, new strategies are required for further improving the detection limit of E-DNA biosensor.

In the present work, we proposed a new strategy for the rapid screening and detection of chlorinated benzenes with significantly sensitive feedback and high selectivity. This strategy could magnify the detection signals by using redox-active MB as indicator (Liu and Barton, 2005; Wong and Gooding, 2007), and minimize the co-existing interferences owning to the high selectivity of the oligonucleotide for chlorinated benzene and the relatively low redox potential of MB (typically −0.25–0 V). As one of the most common POPs in environment, HCB was chosen as a model analyte to systemically study the performance of the new E-DNA biosensor. The proposed E-DNA biosensor displayed concentration-dependant response for HCB, and an extremely low detection limit was achieved. The E-DNA biosensor was further used to systematically screen different chlorinated benzenes. The results demonstrated that the E-DNA biosensor could specifically differentiate these chlorinated benzenes from those co-existing chemicals (citrate, sodium oxalate, ethyl acetate, etc.). The interaction mechanism of the E-DNA biosensor with chlorinated benzenes was also characterized by UV–vis spectrometry and EQCM. The proposed biosensor proved to be a promising "alarm" tool for rapid screening of water and other environmental samples caused by emergent chlorinated benzene contamination.

2. Materials and methods

2.1. Materials and solutions

6-Mercapto-1-hexanol (MCH) was provided by J&K Chemical Ltd. (Sweden). Chlorinated benzenes and other reagents were of analytical reagent grade and purchased from Sigma (USA). Chlorinated benzenes were dissolved in a solution of H_2O and N,N-dimethylformamide (v:v, 4:1) to obtain a series of standard solutions. The thiol-terminated DNA probe 5′-SH-$(CH_2)_6$-AGCTGCGTCACGCCCA-3′ (the DNA oligonucleiotide is from clone RP3-402G11 gene of human DNA sequence), complementary target 5′-TGGGCGTGACGCAGCT-3′, and dsDNA 5′-AGCTGCGTCACGCCCA-3′/5′-TGGGCGTGACGCAGCT-3′ were synthesized by Takara Biotechnology Co. Ltd. (Dalian, China). Stock solutions of the oligonucleotides were dissolved in 20 mmol L^{-1} Tris–HCl (pH 8.0) containing 100 mmol L^{-1} $MgCl_2$, and kept in the refrigerator at −20 °C. Milli-Q water (18 MΩ cm) was used throughout all experiments. Unless otherwise noted, 10 mM pH 7.0 phosphate buffer solution (PBS, 50 mmol L^{-1} NaCl) containing 10 μmol L^{-1} MB (denoted as "MB solution") was used as the electrolytes in all electrochemical experiments.

2.2. Apparatus

Cyclic voltammetry and differential pulse voltammetry (DPV) were carried out on gold electrodes (diameter, 2 mm) using a CHI 440 Electrochemical Workstation (CHI Instruments Inc., USA). A three-electrode system consisted of a single-stranded DNA modified Au electrode (ssDNA/Au) or dsDNA/Au as the working electrode, an Ag/AgCl as the reference electrode (KCl concentration: 3 mol L^{-1}) and a platinum wire as the auxiliary electrode throughout the CV and DPV experiments. 8.0 MHz AT-Cut quartz crystals (diameter, 13.7 mm) with gold evaporated (diameter, 5.11 mm) on both sides were also purchased from CHI Instruments Inc., USA. Absorption spectroscopy was detected by UV–vis spectrophotometer (SP-1901, China).

2.3. Preparation and characterization of ssDNA/Au and dsDNA/Au electrode

The gold electrode surface was mechanically polished with slurries of alumina (1, 0.3, and 0.05 μm diameter successively) and washed ultrasonically with Milli-Q water and ethanol. Then, it was electrochemically cleaned in 1 mol L^{-1} H_2SO_4 by potential scanning between 0 and 1.7 V until a reproducible cyclic voltammogram (CV) was obtained. To obtained good cyclic voltammetric responses of the ssDNA/Au and dsDNA/Au, the concentrations, pH, temperature and reaction times were optimized in control experiments. The cleaned gold electrode was immersed in 15 μL 2 μmol L^{-1} thiolated DNA solution for 6 h at room temperature to obtain the ssDNA/Au. Then the ssDNA/Au was rinsed with 10 mmol L^{-1} PBS and deionized water to remove the physically adsorbed DNA. The ssDNA/Au was then immersed in 1 mmol L^{-1} MCH for 1 h to block the uncovered gold electrode surface.

The dsDNA/Au was prepared by pipetting 15 μL 2 μmol L^{-1} complementary DNA onto the ssDNA/Au, and kept for 2 h to perform DNA hybridization at room temperature. Subsequently, the obtained dsDNA/Au was washed with 10 mmol L^{-1} PBS and deionized water. The dsDNA/Au was stored in 10 mmol L^{-1} PBS solution at room temperature until in use.

The prepared ssDNA/Au or dsDNA/Au was characterized by electrochemical scanning in MB or $[Fe(CN)_6]^{3-}$ solution to monitor the hybridization reactions. Cyclic voltammetry was carried out on the ssDNA/Au or dsDNA/Au from −0.5 to 0 V at 100 mV s^{-1} in MB solution. The same procedure as above was applied in the 2 mmol L^{-1} $[Fe(CN)_6]^{3-}$ containing 500 mmol L^{-1} KNO_3 except for the scan range from −0.1 to 0.6 V.

2.4. Detection and screening of chlorinated benzene with dsDNA/Au biosensor

Taking HCB as an example, the detection was performed by placing 20 μL different concentrations of HCB standard solution onto the surface of the dsDNA/Au for 15 min. Subsequently, cyclic voltammetric scans were performed on the dsDNA/Au biosensor in MB solution to obtain the response signal.

More than 10 kinds of chemicals were screened by dsDNA/Au biosensor at a certain concentration, including different chlorinated benzenes. For a better comparison of these tested compounds, the decrease percentage of peak current (D_{pc}) is very useful to evaluate these analytes (Liu et al., 2009). The D_{pc} was calculated as follows: $D_{pc} = [(i_{MB} - i_t)/i_{MB}] \times 100\%$, where i_{MB} and i_t was the peak current of dsDNA/Au biosensor in MB solution before and after treatment with the analyte. The potential toxicity of analyte was also estimated by comparing the D_{pc} of different analytes.

2.5. UV–vis and EQCM characterization of the interaction between dsDNA and HCB

UV–vis spectra of MB, dsDNA and HCB solutions were recorded from 190 to 700 nm in a quartz cuvette, respectively. 2 mL 10 μmol L^{-1} MB solution was first scanned by the UV–vis spectrometer, then 6 μL dsDNA solution (100 μmol L^{-1}) was injected into the above MB solution, finally 2–10 μL HCB solution (10 mmol L^{-1})

was injected into previous solutions to record the resulting UV–vis spectra.

The dsDNA was immobilized on the gold surface of the AT-Cut quartz crystals as described for the dsDNA/Au. Then 200 μL 10 mmol L^{-1} PBS containing 10 μmol L^{-1} MB was injected into the sensor cell of the EQCM. Finally, 10 μL 1 μmol L^{-1} HCB was added into the above sensor cell, and the reaction process was monitored for 20 min by EQCM.

2.6. Safety considerations

Benzene derivatives are potential carcinogenic agents. MSDS information for these chemicals should be consulted, and precautions should be taken for handling them. Caution must be taken (i.e., wearing gloves, glass and mask), since the vapor of chlorinated benzenes are corrosive to the eyes and skin.

3. Results and discussion

3.1. Characterization and hybridization detection of dsDNA/Au

The hybridization efficiency played an important role in the sensitivity and selectivity of the designed biosensors. In this study, the hybridization process was monitored in $[Fe(CN)_6]^{3-}$ and MB solution, respectively. Fig. 1A displayed cyclic voltammetric signals of $[Fe(CN)_6]^{3-}$ on the bare gold electrode (a), the ssDNA/Au (b), MCH blocked ssDNA/Au (c), and dsDNA/Au (d) in 10 mmol L^{-1} PBS containing 2 mmol L^{-1} $[Fe(CN)_6]^{3-}$. A pair of obvious redox peaks, which could be ascribed to $[Fe(CN)_6]^{4-}/[Fe(CN)_6]^{3-}$ transformation, were observed on the bare gold electrode (Fig. 1A(a)). The shape of the curve (a) and 60 mV peak separation between the cathodic and anodic peak were indicative of the electrochemically reversible one-electron redox process (Porter et al., 1987). Because of the electrostatic repulsive interactions between the negatively charged DNA and $[Fe(CN)_6]^{3-}$, $[Fe(CN)_6]^{3-}$ could not bind to the ssDNA/Au or intercalate into dsDNA/Au (Kelley et al., 1997). Once the gold electrode surface was covered by thiol-terminated ssDNA or dsDNA, $[Fe(CN)_6]^{3-}$ can not be redoxed on the ssDNA/Au or dsDNA/Au electrode. Compared to bare gold electrode (curve a), the cyclic voltammetric signal of $[Fe(CN)_6]^{3-}$ on the ssDNA/Au (curve b) was much lower, and the peak current of $[Fe(CN)_6]^{3-}$ decreased more than 99%, implying that the gold electrode surface was compactly covered by the thiol-terminated ssDNA. The redox peaks of $[Fe(CN)_6]^{3-}$ further decreased when the ssDNA/Au was subsequently blocked with the MCH and hybridized with complementary DNA (Fig. 1A, curve c and d), indicating that a compact-packed self-assembly monolayer of dsDNA and MCH formed at the gold electrode.

The DNA hybridization process was further monitored in MB solution by DPV (DPV is a more sensitive electrochemical method than CV method). MB is an organic dye that belongs to the phenothiazine family and is a redox indicator with the formal potential of about −0.2 V (versus SCE) in neutral solution. It had been reported that MB bind in a different way with ssDNA and dsDNA (Kerman et al., 2002). MB as indicator molecule could bind specifically to the free guanine bases of ssDNA, or readily intercalate into dsDNA (Erdem et al., 2000; Jin et al., 2007). Different binding modes (above mentioned) of MB with ssDNA and dsDNA resulted in variation in electrochemical responses of ssDNA/Au before and after hybridization with complementary DNA. Fig. 1B displayed the DPV signals of ssDNA/Au (curve a) and dsDNA/Au (curve b) electrode in MB solution, in which the reduction peak of MB was monitored at the potential range of −0.25–0 V. There was a sharp peak of MB at −0.125 V on the ssDNA/Au electrode (curve a). Compared to ssDNA/Au, the DPV peak of MB on the dsDNA/Au decreased obviously. This was due to after hybridization, the guanine residues of ssDNA became inaccessible for MB, and only those MB molecules that intercalated into dsDNA can achieve redox on the dsDNA/Au electrode (Boon et al., 2003). There was no obvious peak when the dsDNA/Au (curve c) was scanned in 10 mmol L^{-1} PBS in the absence of MB, as shown in Fig. 1B. The peak current of ssDNA/Au

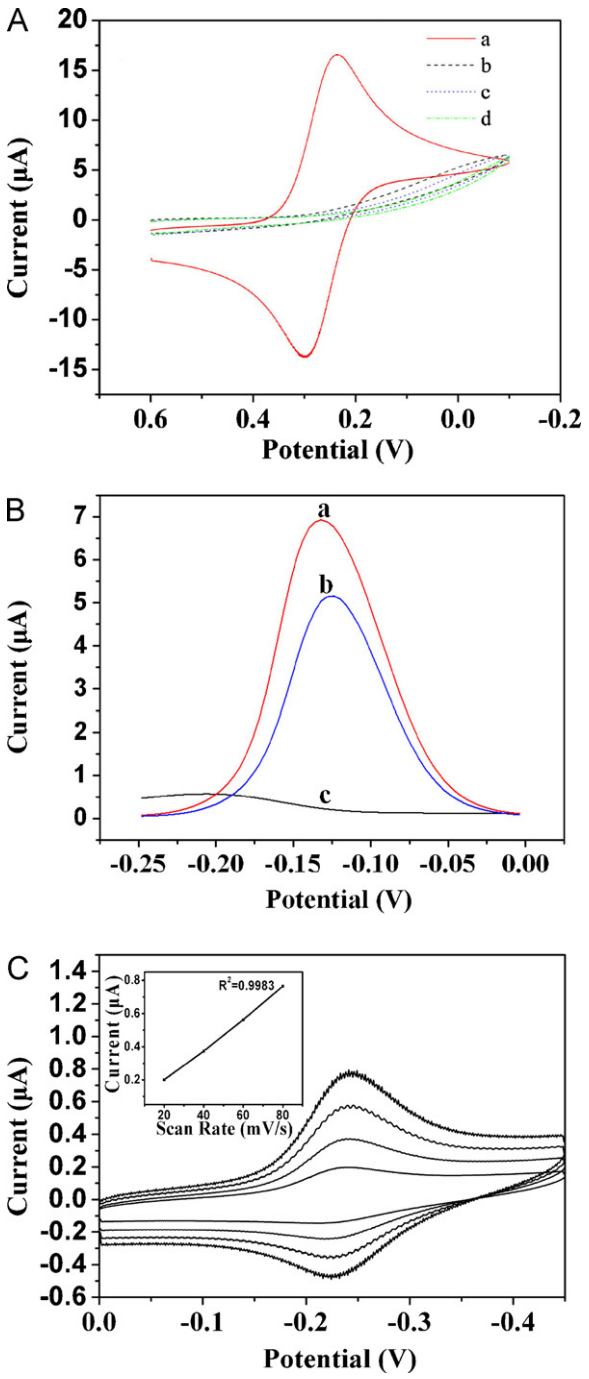

Fig. 1. (A) Cyclic voltammograms of bare gold electrode (a), ssDNA/Au (b), MCH blocked ssDNA/Au (c), and dsDNA/Au (d) in 10 mmol L^{-1} PBS (pH 7.0, 0.5 mol L^{-1} KNO_3) containing 2 mmol L^{-1} $[Fe(CN)_6]^{3-}$. Scan rate, 100 mV s^{-1}. (B) Differential pulse voltammograms of the ssDNA/Au in 10 mmol L^{-1} PBS (pH 7.0) containing 10 μmol L^{-1} MB before (a) and after (b) hybridization with 2 μmol L^{-1} complementary DNA. Curve (c) is the response signal of dsDNA/Au in PBS in the absence of MB. Differential pulse voltammetry conditions: Pulse amplitude, 50 mV; pulse period, 0.2 s. (C) Cyclic voltammogram of dsDNA/Au after incubation of 10 μmol L^{-1} MB in 10 mmol L^{-1} PBS buffer (pH 7.0). Scan rate from inner to outer: 20, 40, 60, 80 mV s^{-1}. Inset: Plot of reduction peak current versus scan rate.

and dsDNA/Au increased sharply in the presence of MB, indicating that MB bound to the ssDNA/Au or intercalated into dsDNA/Au can readily achieve redox (electron transfer). The CV of dsDNA/Au in MB solution with different scan rates was shown in Fig. 1C. With the increase of the scan rates, the cathodic and anodic peak currents of MB increased linearly with the scan rates from 20 to 80 mV s^{-1}, as shown in the inset of Fig. 1C. This revealed that the electron transfer between MB and Au electrode was a surface-controlled electrochemical process, and MB could tightly intercalate into the dsDNA. The above electrochemical response of MB on dsDNA/Au indicated that electron transfer over through the double helix was remarkably efficient (Boon et al., 2003; Ziolkowski et al., 2010).

3.2. Electrochemical screening and detection of HCB and its homologues by dsDNA/Au

HCB is one of the most common environmental pollutants and carcinogens, and its biological toxicology and environmental behavior have been extensively studied (Zhang et al., 2008). Both dsDNA/Au and ssDNA/Au can be used to detect analytes. However, the electrochemical signal of ssDNA/Au is not as stable as dsDNA/Au for the detection of target chemicals based on our experimental data. As is well known, the double helix structure of dsDNA is stabilized by hydrogen bonds in the bases. So dsDNA is more rigid and stable than ssDNA, and ssDNA is more sensitive to the effect of outer environment than dsDNA. Based on the above reason, dsDNA/Au was chosen to detect the target chemicals. Different concentrations of HCB were detected by the dsDNA/Au, respectively. The interaction between HCB and dsDNA was electrochemically magnified by redox-active MB molecules. It should be noted that the reduction potential of MB was at about −0.125 V, where interferences were minimized. A compact-packed self-assembly monolayer of dsDNA and MCH formed on the gold electrode surface, which prevented potential interferents from getting close to the electrode surface. Using the above strategy, more sensitive and selective detection can be achieved for environmental pollutants. Fig. 2A showed the D_{pc} of dsDNA/Au biosensor for the detection of various concentrations of HCB. With the increase of HCB concentration from 100 pmol L^{-1} to 1 μmol L^{-1}, the response signal of MB on the dsDNA/Au biosensor successively decreased. With the increase of HCB concentration from 100 pmol L^{-1} to 1 μmol L^{-1}, the response signal of MB on the dsDNA/Au biosensor successively decreased. As shown in Fig. 2B, the D_{pc} of the dsDNA/Au had a linear relationship with the logarithm value of HCB concentration, ranging from 100 pmol L^{-1} to 100 nmol L^{-1}. The detection limit (S/N = 3) of HCB achieved 30 pmol L^{-1} (about 8.6 ng L^{-1}), which was the lowest value so far reported, far lower than those ever reported for pollutants detection (Rodriguez-Mozaz et al., 2006; Wang et al., 1996). As a biosensor aiming at screening of pollutants, one of the most important performances of the biosensor was the detection limit as the amounts of environmental pollutants are usually at trace level. In previous report, the oxidation signals of guanine bases were used to detect environmental pollutants with affinity for DNA (Rodriguez-Mozaz et al., 2006). The high oxidation potential of guanine (typically 1.0–1.2 V) and the limited number of guanine bases on these types of electrode restrict the improvement of their detection limit, and only mg L^{-1} level of detection limit was obtained. In this study, the low working potential (−0.25–0) can minimize the possible interferences by avoiding the usage of high working potential. The signal magnification strategy through MB indicator plus the low working potential significantly improved the detection limit of the designed biosensor (ng L^{-1}). The good detection limit of the E-DNA biosensor enabled it to be a promising "alarm" tool for rapid screening of chlorinated benzenes on site.

Fig. 2B illustrated the comparison of the D_{pc} of chlorobenzene (CB), 1,2-dichlorobenzene (1,2-DCB), 1,2,4,5-tetrachlorobenzene (1,2,4,5-TCB) and HCB. As shown, with the increasing concentrations of chlorinated benzene, the D_{pc} increased accordingly. Besides, with the increase of chlorine atom number in chlorinated benzene (at the same concentration), the corresponding D_{pc} also increased. The toxicities of chlorinated benzenes could be predicted by the quantitative structure-activity relationship (QSAR) approach based on the photobacterium phosphoreum. Previous studies revealed that the octanol:water partition coefficients ($\log K_{ow}$) was correlated well with the toxicity of these chemicals (Zeng et al., 2008). The order of $\log K_{ow}$ was HCB (5.10) > 1,2,4,5-TCB (4.52) > 1,2-DCB (3.55) > CB (2.86), and the toxic effects of the above chemicals showed a good consistency with the values of $\log K_{ow}$ (Furay and Smith, 1995). The D_{pc} of these chlorinated benzenes on the biosensor fitted well with the toxicity of these analytes, indicating that the proposed dsDNA/Au biosensor might be potential for the toxic effect evaluation of these analytes. The E-DNA biosensor proved to be promising for predicating the potential toxicity of these chemicals, although it might not be very precise.

3.3. Characterization of the interaction mechanism between dsDNA/Au and HCB

Using HCB as a model analyte of chlorinated benzenes, the interaction mechanism between HCB and dsDNA was systematically characterized by electrochemical method, UV–vis spectrometry and EQCM. According to the previous studies, DNA-mediated charge transport relied on the integrity of the bridging π-stack (Cohen et al., 2005; Hihath et al., 2005; Kelley and Barton, 1999). The studies by Boon also demonstrated that efficient charge transport in thiol-terminated DNA self-assembly films is not dependent on direct contact with the gold surface but requires intercalation of the redox probe (i.e. MB), and is mediated by the π-stack of DNA base pair array (Boon et al., 2003). The response signal of MB on the dsDNA/Au decreased sharply upon the dsDNA/Au biosensor was used to detect HCB (Fig. 2 and Scheme 1), which should be ascribed to the release of partial MB from the dsDNA intercalation sites to the solution accompanying the addition of HCB. There are two possible interaction mechanism of the E-DNA biosensor with HCB, as illustrated in Scheme 1: First, because of the strong interaction (π-stacking, hydrogen bond and hydrophobic interaction force) between dsDNA and HCB, those MB molecules intercalated into dsDNA might be directly replaced with HCB, which resulted in the signal decrease of the biosensor. Second, the hydrogen bonds (especially guanine) and the π-stack of DNA base pairs might be destroyed by HCB, and then the double helix was opened and the intercalated MB was released from dsDNA, which can also result in the signal decrease of the biosensor.

The proposed interaction mechanism was also explored by spectroscopy method. The absorption peaks of UV–vis spectra can be correlated with the types of bonds in a given molecule and are valuable in determining the functional groups within a molecule. A full wavelength scan of free MB in solution revealed the undisturbed absorption peak at 664 nm (Fig. 3A). As the dsDNA was injected into the MB solution, hypochromic effects took place at the MB peak (664 nm) owing to the intercalation of MB into dsDNA. Subsequently, high-concentration HCB was added into the above-mentioned solution, resulting in hyperchromic effects (see the magnified Inset of Fig. 3A). With increasing the concentration of HCB, the hyperchromic effects of MB (664 nm) increased accordingly. HCB do not absorb at the wavelength under study. There were two possible reasons for an increase in absorption after addition of HCB: First, those MB molecules intercalated into dsDNA might be directly replaced with HCB. Second, the hydrogen bonds (especially guanine) and the π-stack of DNA base pairs might be destroyed by HCB, and then the double helix was opened and the intercalated MB was released from dsDNA. Accordingly, the free MB concentration

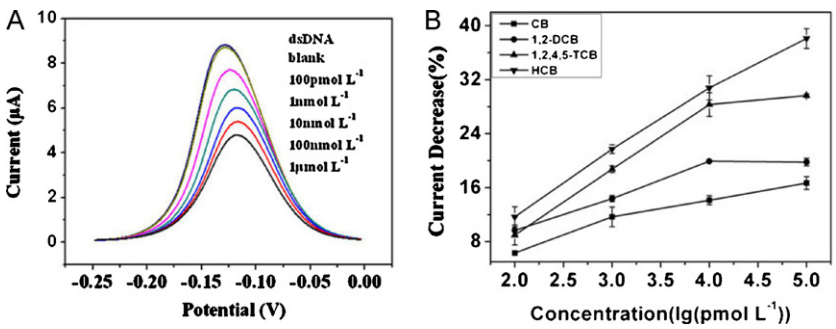

Fig. 2. (A) Differential pulse voltammograms of the dsDNA/Au biosensor for the detection of various concentrations of HCB from 100 pmol L^{-1} to 1 μmol L^{-1}. Pulse amplitude, 50 mV; pulse period, 0.2 s. (B) The D_{pc} of dsDNA/Au for four kinds of chlorinated benzene at different concentrations. They are chlorobenzene, 1,2-dichlorobenzene, 1,2,4,5-tetrachlorobenzene and hexachlorobezene, respectively. The standard deviations are all less than 5%.

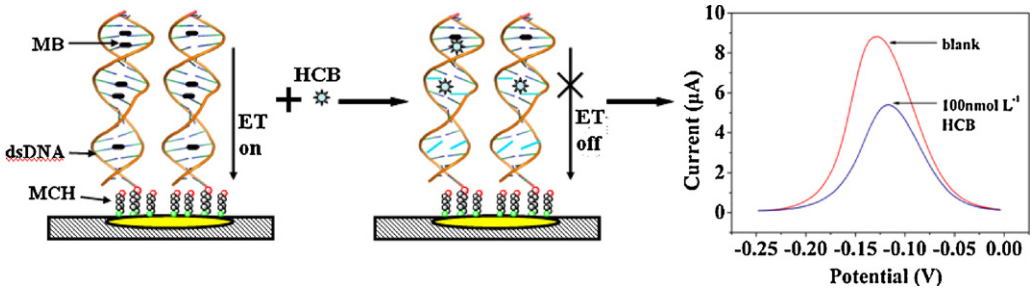

Scheme 1. Schematic diagram of the interaction mechanism between dsDNA/Au biosensor and HCB. The response signal of MB on the dsDNA/Au decreased sharply upon the dsDNA/Au biosensor was used to detect HCB, which should be ascribed to the release of partial MB from the dsDNA intercalation sites to the solution accompanying the addition of HCB.

in solution increased a little, and the resultant absorption peak at 664 nm increased a little (see the local magnification of the UV–vis spectra in the Inset of Fig. 3A). The observed UV–vis spectrometric results were consistent with the electrochemical experimental results.

The interaction mechanism was further investigated by EQCM. The resonant frequency of an oscillating piezoelectric crystal (RFC) can be affected by the change in mass at the crystal surface. The resonant frequency increases with the reduction of mass on the quartz crystal surface. For our quartz crystals, 1.4 ng mass change corresponds to 1 Hz frequency change. It is a very sensitive method for monitoring the addition or reduction of a small mass in thin film systems. The dsDNA was immobilized on the gold surface of the AT-Cut quartz crystals as described for the dsDNA/Au. As shown in Fig. 3B, when HCB was injected into the sensor cell containing 200 μL 10 μmol L^{-1} MB solution, the RFC increased to 24 Hz within 5 min and then kept constant (followed by a slow dynamic equilibrium process). The above results indicated that mass loss have happened on the dsDNA modified AT-Cut quartz crystals. There are two possible reasons for the mass loss: First, some MB molecules intercalated into dsDNA might be replaced with HCB (the molecule weight of MB is larger than HCB). Second, the hydrogen bonds (especially guanine) and the π-stack of DNA base pairs might be destroyed by HCB, and then the double helix of dsDNA was opened and the intercalated MB was released from the dsDNA modified AT-Cut quartz crystals. The EQCM result was also consistent with the UV–vis spectra and electrochemical data (DPV and CV), further confirming the deduced interaction mechanism between DNA and HCB was reasonable. Considering the similar properties of HCB and its homologues, the most possible mechanism of dsDNA/Au biosensor for detection of HCB and its analogues was as follows: First, those MB molecules intercalated into dsDNA might be directly replaced with HCB molecules. Second, the hydrogen bonds (especially guanine) and the π-stack of DNA base pairs might be destroyed by HCB, and then the double helix was opened and the intercalated MB was released from dsDNA.

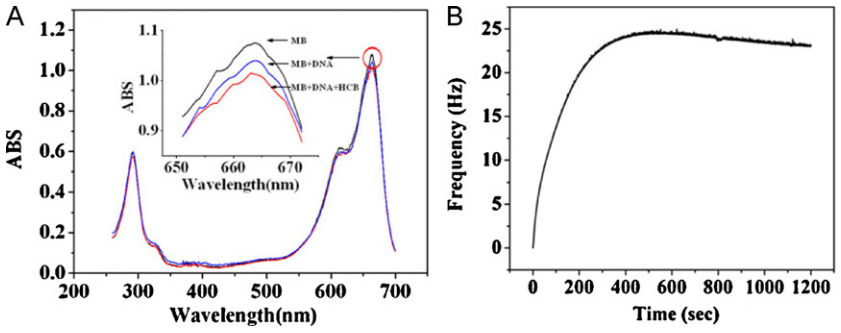

Fig. 3. (A) UV–vis characterization of the interaction between HCB and dsDNA. Inset: The magnified UV–vis spectra from 650 to 672 nm. Buffer solution: 10 mmol L^{-1} PBS (pH 7.0). (B) The frequency shifts observed when the dsDNA modified QCM biosensor was exposed to 1 μmol L^{-1} HCB solution. Supporting electrolyte: 10 mmol L^{-1} PBS containing 10 μmol L^{-1} MB. The positive frequency shift corresponds to the apparent mass decrease.

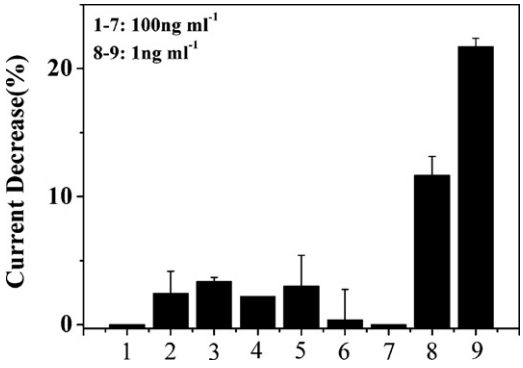

Fig. 4. The D_{pc} of dsDNA/Au biosensor for screening 9 kinds of representative target analytes at different concentrations. Nine kinds of compounds, from 1 to 9, were KNO_3, sodium citrate, sodium oxalate, urea, ethyl acetate, diethyl carbonate, N,N-dimethylformamide, CB and HCB, respectively. The standard deviations are all less than 5%.

3.4. Screening of background interferences and groundwater sample by dsDNA/Au biosensor

Fig. 4 summarizes the DPV responses of dsDNA/Au biosensor for the screening of 9 kinds of analytes. The D_{pc} of dsDNA/Au biosensor for CB and HCB at 1 ng mL^{-1} reached 11.7% and 25.7%, respectively. On the contrary, the D_{pc} of the biosensor for KNO_3, sodium citrate, sodium oxalate, urea, ethyl acetate, diethyl carbonate and N,N-dimethylformamide at 100 ng mL^{-1} was within 5%, respectively. Based on the response signal of different analytes on the E-DNA biosensor, it was defined as a negative screening result when the D_{pc} was less than 5%. On the contrary, it was defined as a positive screening result when the D_{pc} was larger than 5%. So CB and HCB were identified as "positive chemicals" by the E-DNA biosensor and other chemicals mentioned above were identified as "negative chemicals". And a 100-fold excess of "negative chemicals" mentioned above had a negligible effect upon the D_{pc} of the E-DNA biosensor for chlorinated benzene. Besides, the D_{pc} was less than 5%, when the E-DNA biosensor was used for the screening of high concentration of ethanol, phosphate, formamide, dichloroethane, etc. The proposed E-DNA biosensor demonstrated good selectivity for the screening of chlorinated benzenes pollutants in the presence of other high concentration of co-existing interferents.

Table S1 Supplementay Material illustrates the D_{pc} of dsDNA/Au biosensor for screening of relevant natural water samples. The biosensor displayed a negative screening result for the groundwater sample as the D_{pc} was within 3.6%. After the groundwater sample spiked with some amount of CB, 1,2-DCB and HCB, the biosensor showed positive screening results. With the increasing amount of spiked chlorinated benzene, the D_{pc} reached 18.3%, 26.9%, 34.9%, respectively. The real groundwater and spiked groundwater samples were also analysed by GC-ECD and GC–MS. The screening results of the biosensor for groundwater samples were in good agreement with that of gas chromatography. The proposed biosensor proved to be promising for rapid screening of real water samples. Although the E-DNA biosensor was not able to distinguish between HCB and its homologues, it could be used as a useful quick "alarm" for sudden chlorinated benzenes contamination.

4. Conclusion

In the present work, a new strategy based on an E-DNA biosensor was proposed for the rapid screening and detection of chlorinated benzenes pollutants with significantly sensitive feedback and high selectivity. The biosensor displayed concentration-dependant response for HCB with a low detection limit. There were two possible interaction mechanisms of the E-DNA biosensor with HCB: First, HCB might break the hydrogen bonds, open the double helix to release the intercalation MB and disrupt the free guanine to release the MB from guanine bases of ssDNA. Second, the MB intercalation into dsDNA might be replaced with HCB. The biosensor could successfully differentiate chlorinated benzenes from those co-existing chemicals with high specificity. It is interesting to note that the response signal of the biosensor for chlorinated benzenes pollutants were correlative to their respective potential toxicity and concentrations of these analytes. The proposed biosensor proved to be promising as an "alarm" tool for rapid screening of chlorinated benzenes pollutants in real water samples.

Acknowledgment

This work was supported by the Knowledge Innovation Program of the Chinese Academy of Sciences (No DICP K2010C1), the National Natural Science Foundation of China (No 20907051) and the Major State Basic Research Development Program of China (No 2009CB421602).

Appendix A. Supplementary data

Supplementary data associated with this article can be found, in the online version, at doi:10.1016/j.bios.2011.03.027.

References

Ariksoysal, D.O., Karadeniz, H., Erdem, A., Sengonul, A., Sayiner, A.A., Ozsoz, M., 2005. Anal. Chem. 77, 4908–4917.
Boon, E.M., Jackson, N.M., Wightman, M.D., Kelley, S.O., Hill, M.G., Barton, J.K., 2003. J. Phys. Chem. B 107, 11805–11812.
Chen, J.H., Zhang, J., Wang, K., Huang, L.Y., Lin, X.H., Chen, G.N., 2008. Electrochem. Commun. 10, 1448–1451.
Cohen, H., Nogues, C., Naaman, R., Porath, D., 2005. PNAS 102, 11589–11593.
Ding, C.F., Zhang, Q., Lin, J.M., Zhang, S.S., 2009. Biosens. Bioelectron. 24, 3140–3143.
Erdem, A., Kerman, K., Meric, B., Akarca, U.S., Ozsoz, M., 2000. Anal. Chim. Acta 422, 139–149.
Furay, V.J., Smith, S., 1995. Bull. Environ. Contam. Toxicol. 54, 36–42.
Hihath, J., Xu, B.Q., Zhang, P.M., Tao, N.J., 2005. PNAS 102, 16979–16983.
Jin, Y., Yao, X., Liu, Q., Li, J.H., 2007. Biosens. Bioelectron. 22, 1126–1130.
Kelley, S.O., Barton, J.K., 1999. Science 283, 375–381.
Kelley, S.O., Barton, J.K., Jackson, N.M., Hill, M.G., 1997. Bioconjugate Chem. 8, 31–37.
Kerman, K., Ozkan, D., Kara, P., Meric, B., Gooding, J.J., Ozsoz, M., 2002. Anal. Chim. Acta 462, 39–47.
Lin, X.H., Wu, P., Chen, W., Zhang, Y.F., Xia, X.H., 2007. Talanta 72, 468–471.
Liu, T., Barton, J.K., 2005. J. Am. Chem. Soc. 127, 10160–10161.
Liu, S.J., Nie, H.G., Jiang, J.H., Shen, G.L., Yu, R.Q., 2009. Anal. Chem. 81, 5724–5730.
Lucarelli, F., Kicela, A., Palchetti, I., Marrazza, G., Mascini, M., 2002. Bioelectrochemistry 58, 113–118.
Nowicka, A.M., Kowalczyk, A., Stojek, Z., Hepel, M., 2010. Biophys. Chem. 146, 42–53.
Ozsoz, M., Erdem, A., Kara, P., Kerman, K., Ozkan, D., 2003. Electroanalysis 15, 613–619.
Porter, M.D., Bright, T.B., Allara, D.L., Chidsey, C.E.D., 1987. J. Am. Chem. Soc. 109, 3559–3568.
Rodriguez-Mozaz, S., de Alda, M.J.L., Barcelo, D., 2006. Anal. Bioanal. Chem. 386, 1025–1041.
Shin, J.Y., Choi, Y.Y., Jeon, H.S., Hwang, J.H., Kim, S.A., Kang, J.H., Chang, Y.S., Jacobs, D.R., Park, J.Y., Lee, D.H., 2010. Mutagenesis 25, 511–516.
Siddiquee, S., Yusof, N.A., Salleh, A.B., Tan, S.G., Abu Bakar, F., Heng, L.Y., 2010. Sens. Actuators B-Chem. 147, 198–205.
Tombelli, S., Mascini, M., Scherm, B., Battacone, G., Migheli, Q., 2009. Monatsh. Chem. 140, 901–907.
Wang, J., Chicharro, M., Rivas, G., Cai, X.H., Dontha, N., Farias, P.A.M., Shiraishi, H., 1996. Anal. Chem. 68, 2251–2254.
Wong, E.L.S., Gooding, J.J., 2007. J. Am. Chem. Soc. 129, 8950–8951.
Zeng, M., Lin, Z.F., Yin, D.Q., Yin, K.D., 2008. Bull. Environ. Contam. Toxicol. 81, 525–530.
Zhang, L.F., Zheng, M.H., Liu, W.B., Zhang, B., Su, G.J., 2008. J. Hazard. Mater. 150, 831–834.
Ziolkowski, R., Gorski, L., Zaborowski, M., Malinowska, E., 2010. Bioelectrochemistry 80, 31–37.